ELSEVIER

Journal of Nuclear Materials 307–311 (2002) 84–88

journal of nuclear materials

www.elsevier.com/locate/jnucmat

Erosion and re-deposition behavior of plasma facing materials due to tokamak plasma disruption

X. Liu *, Z.Y. Xu, J.M. Chen, L.W. Yan, Y. Liu

Southwestern Institute of Physics, P.O. Box 432, Chengdu 610041, China

Abstract

Plasma irradiation experiments of several kinds of carbon materials and molybdenum were performed in the HL-1M tokamak. The samples emerged into plasma by a depth of 1.5 cm with an angle of 45° between sample surface and magnetic field. After ≈300 plasma discharges with ohmic and NBI heating, melting, microstructure of thin flakes, gas holes and bubbles were found on the surface of molybdenum. No obvious damages were found on the surface of carbon materials, only carbon fibers of 3D-C/C composite were preferentially eroded. Weight changes indicated that most of the samples had little weight loss but few of the samples had large weight increments in which some droplet-shape deposits were found on their surface. Most of the erosion and re-depositions occurred at random on the surface of samples implied that the dominant factor influenced the erosion and re-deposition of plasma facing materials was tokamak plasma disruption.

1. Introduction

Carbon materials and molybdenum are commonly used in current tokamak machines as plasma facing materials (PFMs) and limiter materials. The erosion and re-deposition behaviors of PFMs in tokamak have been intensive studied and many calculation codes have been developed [1]. However, when plasma disruptions happened, the erosion and re-deposition processes became very complicated, some serious damages and re-deposition zones on the surface of PFMs could be founded after a period of operation in tokamak due to large heat loads of plasma disruptions. In situ investigations of the influence on materials are difficult due to the random energy deposition of tokamak plasma disruption. Most of the investigations were carried out by post-mortem analysis or performed in simulated environments; few papers were focusing on the response of PFMs to transient heat loads in tokamak machine [2]. Therefore, it is important to study the erosion and re-deposition behaviors of PFMs and limiter or divetor components caused by plasma disruptions in tokamak environments.

HL-1M is a small scale circular section tokamak with a plasma radius $a = 0.26$ m decided by two poloidal limiters, the limiters and parts of inner wall are covered by high purity graphite and the graphite cover area is about 6% [3]. The previous experiments indicated that no obvious damages were found for carbon-based materials by HL-1M edge plasma irradiation in normal operation conditions [4]. However, when HL-1M operated with high discharge parameters or high power NBI auxiliary heating, plasma disruptions occurred frequently, which gave us a chance to study the edge plasma erosion and re-deposition behaviors of testing materials in tokamak, especially on off-normal operation conditions. In this paper, we will focus on the influence of plasma disruptions on erosion and re-deposition of PFMs.

2. Experimental

The edge plasma irradiation experiment was carried out in HL-1M tokamak, in present experiment, the main

* Corresponding author. Tel.: +86-28 2932225; fax: +86-28 2932202.

E-mail addresses: zhangf@swip.ac.cn, xiang.liu@163.com (X. Liu).

0022-3115/02/$ - see front matter
PII: S0022-3115(02)01177-7

parameters of HL-1M are as follows: $R = 1.02$ m, $a = 0.26$ m, $B_t = 2.5$–3 T, $I_p = 150$–250 kA, pulse duration $t_p \leqslant 1$ s, $n_e \cong 4 \times 10^{19}$ m^{-3}, $T_e(0) \cong 1$ keV. Testing materials are high purity graphite SMF 700, B-doped graphite GB110, 3D-C/C composite, B_4C-doped C/C composite and Mo, Table 1 is their mainly physical properties, detailed description can be obtained in [5], the sample size is $30 \times 9 \times 2$ mm^3. The surface of the samples are polished carefully and cleaned before transferring into vacuum chamber. All 10 samples are arranged in two rows, one row is facing on ion-drift direction, the other is facing on electron drift direction, the angle between sample surface and magnetic field is 45°. The samples were moved into HL-1M vacuum chamber by a magnetic transfer, and the topmost of the sample emerged into plasma by a depth of 1.5 cm, namely on the radial position $r = 24.5$ cm. The electron temperature and density were measured by a Langmiur probes located on the same radial position with samples, Table 2 shows the exposure conditions of target materials, in which the average values (or a range) of located electron density and temperature are listed. In order to avoid the additional sputtering erosion and deposition, the samples were moved backwards to pre-vacuum chamber during He discharge cleaning and wall treating. After about 300 discharges, the samples were moved out of the machine and their weight changes were measured by an electron balance with 1 μg sensitivity, the surface erosion and re-deposition were observed by scanning electron microscopy (SEM) and electron probe microanalyzer (EPMA).

3. Results and discuss

3.1. Weight changes

Figs. 1 and 2 are the weight changes of the samples after exposure of about 300 tokamak discharges. From Fig. 1, we can see that most of the samples have relative little weight loss. Based on the measuring results, the net erosion yield Y_{net} of target materials in tokamak can be indicated as follows:

$$Y_{net} = \Delta m \mathrm{Na}/\rho S V_f n t.$$

Here Δm is the weight loss, Na is atom numbers per volume and ρ is the density of target materials; S is the area exposure to plasma flux direction, $S = 0.675$ cm^2; V_f is ion drift velocity and n is the located average ion density, taking the measuring results of Langmuir probes, $T_i = T_e = 25$ eV, $V_f = (2T_i/m)^{1/2} = 6 \times 10^6$ cm/s, $n = 1 \times 10^{12}$ cm^{-3}, t is the total exposure time, $t = 200$ s. Considering the relative simple erosion process of

Table 1
Main physical properties of the target materials

Materials type	Composition	Density (g/cm^3)	Porosity (%)	Bend strength (MPa)	Thermal conductivity (RT) (W/m K)
SMF700		1.82	49.2	46.6	72.8
GB110	10 wt% B_4C	2.00	6.1	81.1	48.6
3D-C/C		2.03	3.2		197/190
B_4C-C/C	10 wt% B_4C	2.09	3.0		120/118

Table 2
Exposure conditions of target materials in HL-1M edge plasma

Operation mode	Number of discharges/ type of heating		Located plasma parameters		Operation time (s)
	Low parameter ($I_p = 130$–150 kA)	High parameter ($I_p = 190$–210 kA)	Electron density (cm^{-3})	Electron temperature (eV)	
Normal	160/ohmic + LHCD (or ECRH)		1×10^{12}	25	128
		10/ohmic + LHCD (or ECRH)	2×10^{12}	40	7.5
	57/ohmic + NBI		1×10^{12}		40
Disruption	25/ohmic + LHCD (or ECRH)		2×10^{12}	40–80	8
		5/ohmic + LHCD (or ECRH)	4×10^{12}	40–80	1.8
	42/ohmic + NBI		4×10^{12}	40–80	14

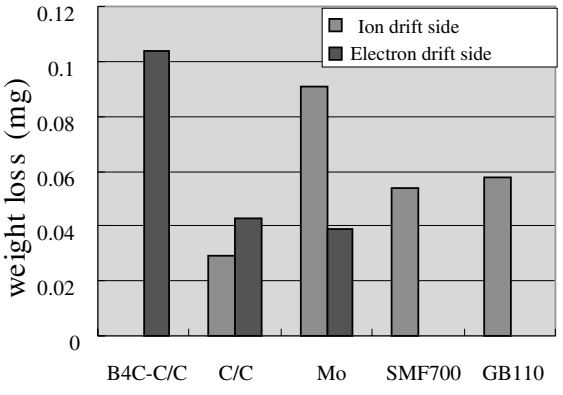

Fig. 1. The weight loss of the samples after about 300 times HL-1M tokamak discharges.

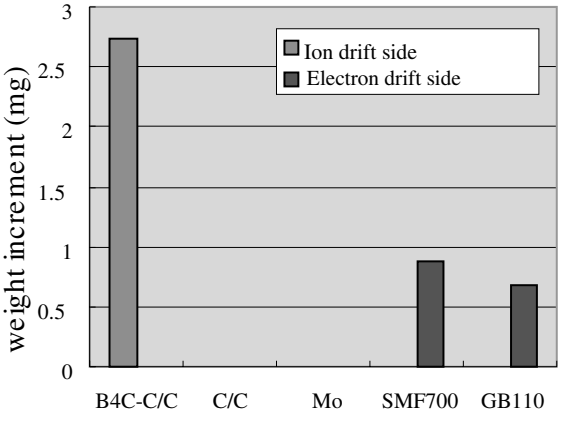

Fig. 2. The weight increment of the samples after about 300 times HL-1M tokamak discharges.

molybdenum on ion drift side (only physical sputtering and re-deposition, see next section), whose weight loss is 9.1×10^{-5} g, as an example, its Y_{net} can be indicated as:

$$Y_{net} = 0.61 \times 10^{-3} \text{ atoms/ion}.$$

In present condition, physical sputtering and re-deposition of impurities have contribution to Y_{net}, calculations based the Monte-Carlo code indicate that the physical sputtering yields of some metal materials, such as Ti and Mo are in the range of 10^{-3} to 10^{-4} atoms/ion for about 25 eV ion temperature and hydrogen plasma [6,7], it seems to be in agreement with present experimental result. But actual physical sputtering yield might be larger than the calculation value owing to the contribution of charge exchange neutrals from main plasma and impurity ions flowing through the edge. On the other hand, the re-deposition of impurities will compensate partly the sputtering erosion, and even offset the sputtering erosion completely in some cases (as shown in Fig. 2). In fact, SPMA analysis indicated that the surface of all samples was covered by Si and Fe, and the concentrations of Si and Fe became higher with far away from core plasma. However, it is difficult to estimate accurately the contribution of re-deposition to weight increments. For carbon materials, the erosion yield should higher than that of molybdenum due to additional chemical sputtering and radiation enhanced sublimation. But present experiment did not display this trend for all carbon materials, one main reason was that the re-deposition rate was relatively higher on the surface of these materials.

In Fig. 2, it shows weight increments of three carbon material samples after plasma exposure in which B_4C doped C/C composite has the largest weight increment, the results indicate that there is not net erosion process for whole limiter surface. The details will be discussed in Section 3.3.

3.2. Plasma erosion

3.2.1. Molybdenum

Some serious damages were found on the top surface of molybdenum sample on electron drift side, part of the topmost surface were melted and most of them became into multi-layer structure of thin flakes as shown in Fig. 3(a). This surface structure could come from plastic deformation at high temperature, and it is somewhat similar with the surface topography of the rolled tungsten exposed to plasma stream by 50–60 shots (plasma pulse length $t = 40$–50 μs) with 1.5 kJ cm^{-2} energy density [8]. Present experimental results imply that there are relative high heat load deposited on the surface of Mo, and its transient surface temperature, at least in the part of the topmost, should be over 2625 °C (melting point of Mo). In order to estimate the target temperature, a experiment for temperature measurement was performed by using the same size Mo target welded a thermocouple. The top of Mo target was placed at the radius of 24–24.5 cm, i.e. being immersed by 1.5–2 cm into the plasma. Results showed that the target temperature was usually in the range of 300–500 °C. Because of bulk temperature insensitive to the transient heat loads, the actual surface temperature should be much higher than the measured value, particularly in the cases of disruptions. Meanwhile, the measurement results of heat flux probes indicated that the located total heat flux density is at the range 200–360 W/cm^2 in normal operation conditions. In fact, the heat flux density on the surface of the samples located on electron and ion drift sides can be estimated as 188 and 79 W/cm^2, respectively. In above calculations, electron density and electron temperature are taken as 2×10^{12} cm^{-3} and 25 eV, respectively. An ion heat transmission coefficient $\gamma_i = 2T_i/T_e$ and an electron heat transmission coefficient

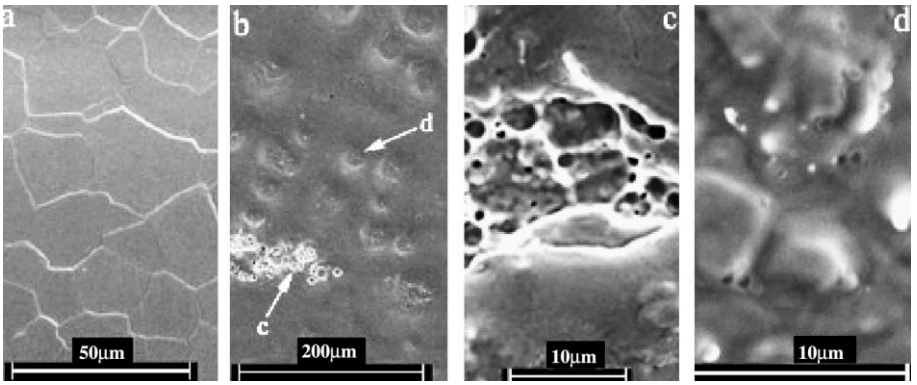

Fig. 3. Photographs of molybdenum on electron drift side by HL-1M plasma irradiation: (a) multi-layer structure of thin flakes, (b) overview of gas holes and bubbles, (c) magnification of 'c' zone in (b), (d) magnification of the 'd' zone in (b).

$\gamma_e = 2/(1-\delta_e) - 0.5\ln[2\pi(m_e/m_i)(1+T_i/T_e)(1-\delta_e)^{-2}]$ are adopted [1]. Here m_e and m_i is electron and ion mass, respectively, δ_e is the secondary electron emission coefficient of the target surface. There are many models to calculate γ_i and γ_e, for simple, $\delta_e = 0$, $T_i = T_e$ are assumed and $\gamma_i = 2$, $\gamma_e = 4.8$ can be obtained. Therefore, molybdenum melting and microstructure changes should not be induced by tokamak normal operations. On the other hand, it was seen that more than the seventh of the ohmic discharges and half of the discharges with NBI auxiliary heating were terminated by hard disruptions from Table 2. Taking the upper limit to electron temperature $T_e = 80$ eV and electron density $n_e = 4 \times 10^{12}$ cm^{-3} for plasma disruption (as shown in Table 2), the heat flux density of Mo on electron drift side will be over 2 kW/cm^2 estimated by the same method above. Although the pulse duration of energy deposition for disruptions is very short (<0.5 ms), relatively high energy deposition has a capability of destruction to target materials.

Behind the surface zone in which melting and the thin flake structure were formed as mentioned above, many circular hollows were observed as shown in Fig. 3(b). Parts of them became dense holes (Fig. 3(c)), and many small bubbles appeared in the inner of most of them (shown in Fig. 4(d)). The diameter and depth of the hollow became smaller with the distance far from the top of the sample. A possible reason was that the concentrations of implantation hydrogen atoms or the residual gas reached the located saturation limitation and they were bursting out under transient high heat loads.

It must be mentioned that all these erosion phenomena appeared on the surface of Mo on electron drift side did not take place on the surface of Mo on ion drift side. The main reason maybe due to the difference of energy deposition on ion and electron drift sides, especially under off-normal operation conditions.

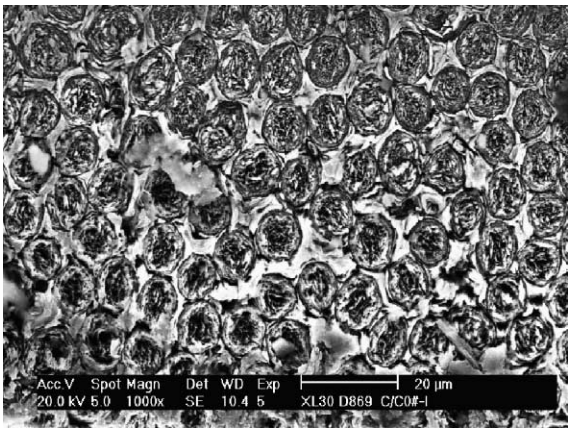

Fig. 4. SEM image of 3D-C/C composite on electron drift side after 300 plasma discharges.

3.2.2. Carbon materials

The erosion and deposition behaviors of all four kinds of carbon materials are quite different and it does not matter whether they are on electron or ion drift sides. Most of them have not suffered to obvious damages except the 3D-C/C sample on electron drift side in which a preferentially erosion of carbon fibers are found on the top surface as shown in Fig. 4. Cracks are also found among the carbon fiber bundles or at the interface of the fiber bundles parallel and normal to the surface. All these phenomena became more and more blurred with the distance far from the core plasma and vanished finally at the position of about 150 μm from the top of the sample. Preferentially erosion of carbon fibers is also found by other authors for B_4C doped C/C composites [9,10]. Here the main reason is due to the difference of thermal conductivity and expansibility between fibers and the periphery. For the C/C composites developed in

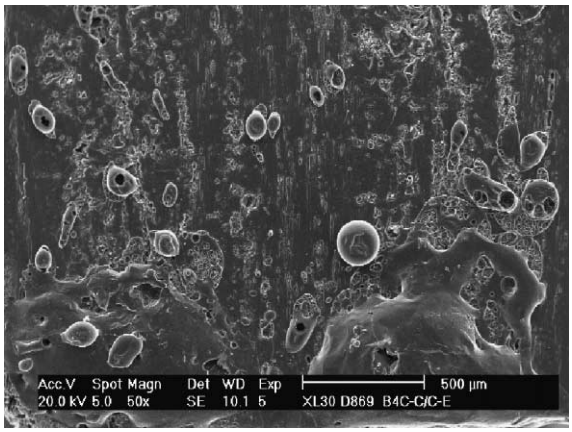

Fig. 5. A view of the deposits on the surface of B_4C-C/C composite sample on electron drift side.

China, the thermal conductivity of fibers is usually lower than that of the periphery graphite.

3.3. Re-deposition

AS mentioned on Section 3.1, impurities from PFMs could re-deposited on the surface of PFMs, especially for the surface unirradiated directly by plasma flux, usually there is net erosion process for the limiter surface. But in the present experiment, three samples showed net weight increase as shown in Fig. 2, surface topography of these samples indicated that there were many droplet-shape deposits on their surface. Fig. 5 is the view of the re-deposition on the top part of B_4C-C/C composite sample on electron drift side, which has a largest weight increment. EPMA analysis indicated that these deposits consisted of silicon, carbon, and small content of calcium, in which the content of iron element is quite lower than the other surface exposure to plasma. Considering stainless steel inner wall structure in HL-1M and siliconization wall conditions, a reasonable explanation is that droplet-like deposits come from the flaking of the wall coating and the splashing of melted silicon coating under plasma disruptions, and just the random plasma disruption phenomena induce undetermined re-deposition behaviors.

4. Conclusions

Firstly, the net erosion yield of molybdenum in present experimental conditions are estimated, relatively low value is mainly come from the contribution of impurity Si and Fe re-deposition on sample surface.

Secondly, owing to the influence of HL-1M tokamak plasma disruptions, all testing samples do not entirely reveal net erosion behaviors, and the erosion and re-deposition behaviors are quite different, some of them cannot be explained by the energy deposition difference between ion and electron drift sides. Therefore, melting, multi-layer structure of thin flakes, gas holes and bubbles were found on the top part of molybdenum surface on electron drift side, but there is nothing for the surface on ion drift side. As to carbon materials, only preferentially erosion of carbon fibers and cracks were observed on the top surface of 3D-C/C composite on the electron drift side. The B_4C-C/C composite sample on ion drift side have the largest weight loss, but the B_4C-C/C composite sample on electron side have the largest weight increment, in which many droplet-like deposits of silicon and carbon mixture were found. It implied that plasma disruptions could play an important role to the erosion and re-deposition behaviors of PFMs in the tokamak environments where plasma disruptions occurred frequently.

Acknowledgement

The author would like to thank Professor Naoaki Yoshida of Kyushu University of Japan for helpful suggestions to bubble formation.

References

[1] P.C. Stangeby, JET Joint Undertaking, G.M. Mccracken, Nucl. Fus. 30(7) (1990) 1225.
[2] H. Bolt, T. Scholz, J. Boedo, K.H. Finken, A. Hassanein, J. Linke, Fus. Eng. Des. 39&40 (1998) 287.
[3] HL-1M team (presented by E.Y. Wang), IAEA 16th Conference Proceedings, Montreal, Canada, 7–11 October, vol. 1 (1996) 693.
[4] X. Liu, Z.Y. Xu, W.Y. Hong et al., China Nucl. Sci. Technol. Report, CNIC/CD/ 2001-3.
[5] Z.K. Shang, Z.Y. Xu, X.W. Deng, X. Liu, N.M. Zhang, Surf. Coating Technol. 131 (2000) 109.
[6] G. Fussmann, U. Ditte, W. Eckstein, et al., J. Nucl. Mater. 128&129 (1984) 350.
[7] B. Lipschultz, B. Labombard, E.S. Marmar, et al., J. Nucl. Mater. 128&129 (1984) 555.
[8] N.I. Arkhipov, V.P. Bakhtin, S.M. Kurkin, et al., Fus. Eng. Des. 49&50 (2000) 151.
[9] T. Yamaki, Y. Suzuki, A. Chiba, et al., J. Nucl. Mater. 241–243 (1997) 1132.
[10] K. Nakamura, M. Dairaku, M. Akiba, Y. Okumura, J. Nucl. Mater. 241–243 (1997) 1142.